Available online at www.sciencedirect.com

ScienceDirect

journal homepage: www.elsevier.com/locate/he

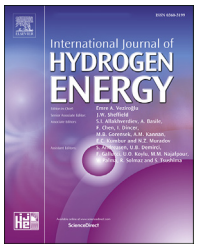

Development and testing of a 100 kW fuel-flexible micro gas turbine running on 100% hydrogen

Reyhaneh Banihabib [a,*], *Timo Lingstädt* [b], *Magnus Wersland* [a], *Peter Kutne* [b], *Mohsen Assadi* [a]

[a] *Faculty of Science and Technology, University of Stavanger, Stavanger, Norway*
[b] *German Aerospace Center (DLR), Germany*

HIGHLIGHTS

- Hydrogen's potential as an alternative, carbon-free fuel for micro gas turbines is assessed.
- The obstacles of utilizing hydrogen fuel in a micro gas turbine are addressed and the necessary modifications are presented.
- Data from successful tests of a micro gas turbine running on hydrogen blends ranging up to 100% hydrogen is presented.
- NOx emissions below the standard limits were achieved with the new setup.
- The study's outcomes could aid researchers and developers in incorporating hydrogen as a carbon-free energy carrier.

ARTICLE INFO

Article history:
Received 28 February 2023
Received in revised form
28 April 2023
Accepted 27 June 2023
Available online 13 July 2023

Keywords:
Micro gas turbine
Hydrogen fuel
Development and test
Clean fuel
Energy transition

ABSTRACT

Hydrogen, as a carbon-free energy carrier, has emerged as a crucial component in the decarbonization of the energy system, serving as both an energy storage option and fuel for dispatchable power generation to mitigate the intermittent nature of renewable energy sources. However, the unique physical and combustion characteristics of hydrogen, which differ from conventional gaseous fuels such as biogas and natural gas, present new challenges that must be addressed.

To fully integrate hydrogen as an energy carrier in the energy system, the development of low-emission and highly reliable technologies capable of handling hydrogen combustion is imperative. This study presents a ground-breaking achievement - the first successful test of a micro gas turbine running on 100% hydrogen with NOx emissions below the standard limits. Furthermore, the combustor of the micro gas turbine demonstrates exceptional fuel flexibility, allowing for the use of various blends of hydrogen, biogas, and natural gas, covering a wide range of heating values. In addition to a comprehensive presentation of the test rig and its instrumentation, this paper illuminates the challenges of hydrogen combustion and offers real-world operational data from engine operation with 100% hydrogen and its blends with methane.

* *Corresponding author.*
E-mail addresses: Reyhaneh.Banihabib@uis.no (R. Banihabib), Timo.Lingstaedt@dlr.de (T. Lingstädt), Magnus.Wersland@uis.no (M. Wersland), Peter.Kutne@dlr.de (P. Kutne), Mohsen.Assadi@uis.no (M. Assadi).

https://doi.org/10.1016/j.ijhydene.2023.06.317

Nomenclature

Alphanumeric Variables

c_p	Specific heat of gas at constant pressure (J/kg K)
$\dot{m}$	Mass flow rate (kg/s)
N	Relative rotational speed [%]
P	Power (kW)
p	Pressure [bar]
T	Temperature (K)
V	Valve position [%]

Greek Symbols

ρ	Density (kg/m3)
φ	Equivalence ratio

Indices

comb	Combustor
f	Fuel
nom	Nominal
norm	Normalized

Abbreviations

AF	Adiabatic Flame
LHV	Lower heating value
MGT	Micro gas turbine
TIT	Turbine inlet temperature
TOT	Turbine outlet temperature

Introduction

Micro gas turbine (MGT) engines with a power output between 3 and 300 kW are instrumental in decentralized power generation, due to their reliability and ability to quickly respond to changes in load, making them an ideal backup option for intermittent renewables [1,2]. Their compact size, lightweight, and low installation and maintenance cost further strengthen MGT's position as a power generator in the future's distributed power system. Today's MGTs can run on a variety of fuels, from high-heating value fuels like methane and natural gas to lower-heating value fuels like biogas.

Despite the fuel-flexibility of MGTs providing a wide range of options, greenhouse gas emissions from carbon-based fuels continue to be a concern. Using carbon-free fuels, such as hydrogen, or carbon-neutral fuels is the most efficient way to achieve zero net CO_2 emissions in an MGT, given the difficulties associated with capturing CO_2 due to its low partial pressure [3]. The shift from the current power generation infrastructure, which primarily relies on carbon-based fuels, necessitates bridging technologies such as fuel-flexible MGTs that can work with blended fuels containing high levels of hydrogen [4].

Hydrogen fuel has the potential to significantly contribute to the shift towards a more sustainable and low-carbon energy system in the heat and power generation sector. The advantage of using hydrogen in power generation is its ability to significantly decrease greenhouse gas emissions and enhance air quality, as it only releases water vapor during combustion, in contrast to traditional fossil fuels like coal and natural gas, which emit harmful pollutants. By using hydrogen as an energy storage solution, excess energy generated from renewable sources can be saved and utilized at a later time, ensuring a consistent and dependable energy supply even when renewable sources are unavailable [5].

Many research and development initiatives have been carried out on both large-scale and small-scale gas turbine units to address the challenges of using pure hydrogen or hydrogen-blended fuels. In 1998, Morris et al. published a paper [6] that presented their findings on incorporating hydrogen into heavy-duty gas turbines that were originally powered by natural gas. According to the authors, adding 10% hydrogen did not impact NOx emissions, but it reduced carbon monoxide production.

Shih et al. [7] conducted a study using computer simulation to evaluate the impact of hydrogen combustion in micro gas turbines. The authors employed computational fluid dynamics to examine the burning features of mixed fuels with different hydrogen volumetric fractions (ranging from 0 to 90%) in a can combustor that was initially designed for natural gas. Several case scenarios were tested to fuel the engine, and the results indicated steady combustion performance. However, the researchers found that modifications to the combustor design were necessary to tackle emissions since the original design was found to be insufficient [7].

In another study by Imteyaz et al. [8], a series of experiments were conducted to investigate the combustion behaviour of hydrogen-enriched methane fuel in a swirl-stabilized type gas-turbine combustor. The researchers increased the amount of hydrogen in the blended fuel up to 80% by volume and derived upper and lower limits for providing air to maintain stable combustion.

Rajpara et al. [9] performed both experimental and numerical investigations to assess the effect of hydrogen injection on a gas turbine with an upward swirl combustor running on methane fuel. The study found that increasing hydrogen content resulted in smaller flame dimensions but higher NOx emissions due to higher flame temperature, as well as a decrease in CO emissions.

Minakawa et al. [10] designed a prototype of a lean premixed swirling flame combustor for a micro gas turbine to operate with pure hydrogen. The combustor was tested at atmospheric pressure and demonstrated high combustion efficiency and low NOx emissions. It was then installed on a micro gas turbine to assess its performance in actual conditions. During engine startup, flashbacks were observed which had not been seen in previous component tests. By controlling the airflow to the combustor, the flashbacks were prevented, and the engine achieved self-sustaining operation. The results of the study confirmed the excellent combustion performance of the micro gas turbine, including heat release rate, combustion efficiency, and low NOx emissions in lean conditions [10].

Cappelletti et al. [11] conducted a study to investigate the combustion of pure hydrogen in a lean premix burner using both experimental and numerical simulation methods. The experimental setup was based on a pre-existing burner from a heavy-duty gas turbine and was modified to allow for variable premixing levels. The study found that to avoid flame positioning inside the premix duct, high flow velocity was required during hydrogen combustion. The results indicated the potential for developing combustion technology using

pure hydrogen fuel while maintaining emissions within the regulated limits.

In May 2020, Kawasaki successfully tested an industrial gas turbine with hydrogen fuel using their dry low emission combustion technology. The combustor employs micro-mix combustion technology that utilizes ultra-small hydrogen-fueled flames and achieves low NOx combustion without the need for water or steam, which is beneficial in terms of cycle efficiency [12,13].

In this paper, the process of transforming a commercial micro gas turbine to run on blended methane/hydrogen fuel is outlined in detail. The project began in September 2021 in Stavanger, Norway, where a 100-kW micro gas turbine was modified to operate on a blend of hydrogen and methane. During the first phase, a hydrogen content of up to 30% on a volume basis was achieved, leading to unstable operation due to combustion instabilities at high power rates. The findings from phase 1 can be found in Ref. [14]. In the second phase, the combustion chamber and fuel control system were reengineered to handle higher hydrogen content and operate at higher power rates. All the modifications made to the system are described and illustrated in the paper. The engine was run on 100% hydrogen fuel and produced NOx emissions below regulatory standards, as demonstrated by the data collected from the sensors, which is presented in the paper.

In the following sections, first, the main challenges of the work are described, followed by the methods and approaches to overcome them. Lastly, the experimental results from running the MGT with a high hydrogen content of up to 100% are presented and discussed. Throughout the article, the content of hydrogen is presented as percentages of the whole fuel based on volume.

Challenges of running an Mgt with hydrogen

The transformation of a gas turbine engine, including MGTs, to run on alternative fuels presents numerous challenges. The unique characteristics of hydrogen combustion require adjustments to both the combustor and other components of the system to ensure secure and stable operation while adhering to emission regulations. The difficulties associated with operating MGTs with hydrogen or hydrogen-blended fuels can be categorized into two distinct areas.

- The change in combustion properties of hydrogen compared to traditional fossil fuels, which affects the design and function of the combustor, i.e., challenges at the component level.
- Challenges related to the modification of the flow characteristics as a result of variations in combustion products and their impact on engine performance, i.e., challenges at the system level.

In this section, an overview of those challenges is provided.

Component-level complications

Provided in Table 1 is an outline of the physical and chemical properties of hydrogen and methane, serving to contrast the combustion characteristics of hydrogen fuel. Variations in these properties create differences in combustion characteristics between the two fuels, necessitating distinct combustor designs. Developing combustor technology for hydrogen combustion becomes even more complex when the objective is to operate with both pure hydrogen and hydrogen-blended fuels.

The hydrogen molecule has a light weight and a broad flammability range, which makes it suitable for use in gas turbine engines. It has the ability to burn in a mixture with an equivalence ratio of 0.1 in lean conditions, and up to 7.1 in rich conditions, allowing for a wide range of power outputs at different air-fuel ratios. The values presented in Table 1 are under atmospheric conditions, however, it is important to note that the lower limit of flammability increases under high-pressure conditions and decreases with higher temperatures. As a result of these opposing effects, the lower flammability limit of hydrogen in a micro gas turbine is higher than 0.1 but lower than methane under the same thermodynamic conditions, according to Ref. [16].

Hydrogen and methane have a significant difference in their minimum required ignition energy, with hydrogen being about 10 times lower in atmospheric conditions than methane. This high ignition temperature of methane and its slow flame propagation temperature can pose difficulties in ignition and maintaining stable combustion in low-load ranges of gas turbines. The addition of hydrogen holds the potential in enhancing combustion performance with regard to efficiency and stability as shown in studies [8,17–20]. It has been observed that an increase in the hydrogen share results in an increase in laminar burning velocity [21]. This is expected to result in a more stable flame, reducing the risk of flame-out in lean combustion conditions [22]. The broad flammability limits, high flame speeds, and low required ignition energy of hydrogen make it beneficial for hydrogen engine efficiency. Researchers have found that using hydrogen as a supplementary fuel to hydrocarbons can enhance the ignitability and flammability of lean premixed combustors and potentially allow for stable lean burn at lower temperatures [17,18]. Blending hydrogen with hydrocarbon fuels has the potential to improve flame stability in lean conditions with low temperatures, which in turn could help to reduce NOx emissions [18,19].

The laminar flame speed, which is an indicator of the burning rate, can have a significant impact on combustion

Table 1 – Comparison of the properties of hydrogen and methane in atmospheric pressure and 300 K temperature [15].

Property	Methane	Hydrogen
Molecular weight	16.04 g/mol	2.02 g/mol
Density	0.65 kg/m^3	0.08 kg/m^3
Lower heating value (per mass)	50 MJ/kg	120 MJ/kg
Stochiometric air/fuel ratio	17.1 kg/kg	34.2 kg/kg
Minimum ignition energy	0.28 mJ	0.02 mJ
Flammability limits	0.5 ~ 1.67	0.1 ~ 7.1
Stoichiometric air-to-fuel ratio (kg/kg)	17.1	34.1
Stoichiometric air-to-fuel ratio (kmol/kmol)	59.7	2.4

efficiency and serves as the basis of turbulent combustion. In essence, the laminar flame speed represents the propagation rate of the flame front relative to the unburned mixture. Determining values for laminar flame speeds can provide validation targets for chemical kinetic models or be used in turbulent combustion models [20].

Zhou et al. [23] conducted numerical and experimental investigations to study the effect of fuel composition on combustion kinetics, for different equivalence ratios (0.6–1.5) and pressures (0.1–0.5 MPa), with a wide range of H_2/CO/CH_4 compositions. Their research showed that increasing the H_2 content in the fuel significantly promotes fuel reaction activity, which in turn increases the laminar flame speed. Additionally, the study found that increasing pressure resulted in a reduction in flame speed.

The addition of hydrogen to the fuel mix also results in a change in the adiabatic flame temperature, which increases as the hydrogen content increases [23,24]. The temperature will rise with the equivalence ratio (φ) until reaching its peak, which occurs in slightly rich conditions ($\varphi \approx 1.05$). Beyond that point, the adiabatic flame temperature decreases as the mixture becomes richer because the specific heat value of the combustion products decreases at a faster rate than the heat release rate. The introduction of hydrogen into a methane mix will cause an increase in the adiabatic flame temperature [22] as hydrogen will speed up the reaction rate [25].

The production of toxic nitrogen oxides, also known as thermal NOx formation, is a concern in combustion processes with high flame temperatures. The oxidation of nitrogen molecules in the air occurs as the fuel burns at high temperatures, leading to the formation of NOx. Research has shown that a significant amount of NOx formation occurs around 1800 K and the rate of production increases rapidly with further temperature rise [26].

In gas turbines that use hydrocarbon-based fuels, the problem of high flame temperatures is addressed by premixing the fuel with air before combustion, thereby keeping the flame temperature below a certain value without affecting efficiency [27]. This approach is known as lean premixed burners or dry low NOx burners, which however, face several critical issues during fuel premixing, such as combustion instabilities, flashbacks, extinction, and thermo-acoustic instabilities [28,29].

The utilization of hydrogen or hydrogen-enriched fuels in gas turbines requires rethinking the design of the combustors, due to the large differences in flammability range and reaction rates between hydrogen and hydrocarbons [30]. The quick ignition of hydrogen before adequate premixing with air will result in high flame temperatures, promoting NOx formation.

Another aspect to consider when examining the effects of hydrogen addition to fuel is its impact on CO emissions. Carbon monoxide production in a gas turbine is primarily a result of the incomplete combustion of hydrocarbon fuel and is therefore inversely proportional to the flame temperature [31]. It is believed that the addition of hydrogen to the fuel blend will result in a decrease in CO emissions because there will be fewer carbon elements present and the flame temperature will be higher in the presence of hydrogen, given that the equivalence ratios are the same in both cases [32].

System-level complications

The properties of hydrogen and methane, which are distinct from each other, have an influence on the combustion behaviour as previously discussed. Variations in fuel flow rate are expected as a result of differences in heating value and density between the two fuels. In addition, the altered flow properties resulting from the different combustion products could potentially have an impact on the thermodynamics of the MGT cycle, as outlined in Refs. [33,34].

To assess the impact of the difference in properties between hydrogen and methane on the combustion characteristics, a comparative assessment is carried out based on the design point of the cycle. This assessment is performed by running the MGT at baseload and ISO conditions. The flue gas properties are analysed over a range of equivalence ratios for both methane and hydrogen combustion using Cantera software [35]. The air is mixed with the fuel in different equivalence ratios while keeping the pressure constant. This mixture equilibrates at 21% oxygen and 79% nitrogen, with a pressure of 4.3 bar and a temperature of 610 K. The results of these calculations are shown in Fig. 1, which illustrates the adiabatic flame temperature, the specific heat capacity at constant pressure, and the density of the flue gas for both fuels. The results show that the differences in flue gas properties between methane and hydrogen combustion become more pronounced as the mixture becomes richer.

In theory, the combustion process of methane will result in the production of steam and carbon dioxide which will then be mixed with the water and nitrogen content in the air, as described in Eq. (1). On the other hand, the combustion process of hydrogen will result in the production of only steam, as described in Eq. (2).

$$CH_4 + 2(O_2 + 3.76N_2) \rightarrow CO_2 + H_2O + 7.52N_2 \quad (1)$$

$$2H_2 + (O_2 + 3.76N_2) \rightarrow 2H_2O + 3.76N_2 \quad (2)$$

In reality, the combustion process of both methane and hydrogen fuels can result in the production of toxic nitrogen oxides, carbon monoxides, and other radicals, which can alter the composition and properties of the flue gas produced. To account for these factors, a computational tool known as Cantera is used to calculate the chemical potential of each element present in the flue gas [35]. The tool uses a mixture of fuel and air and sets it to a state of chemical equilibrium. It then employs a stoichiometric algorithm to determine the intermediate states that meet the constraints of each element, though they are not necessarily in a state of chemical equilibrium [35].

In Fig. 1, the differences in the flue gas properties are shown to be closely related to the equivalence ratio. To determine the conditions that exist in the current MGT, it is necessary to evaluate the value of the equivalence ratio. To produce 100 kW of power with 30% efficiency, the fuel flow rate is calculated based on the heat input required. Using 50 MJ/kg of lower heating value (LHV) for methane, 6.7 g/s of methane is needed and an equivalence ratio of 0.14 is achieved. The adiabatic flame temperature of the flue gas under these conditions is recorded as 1230.5 K, with a density of

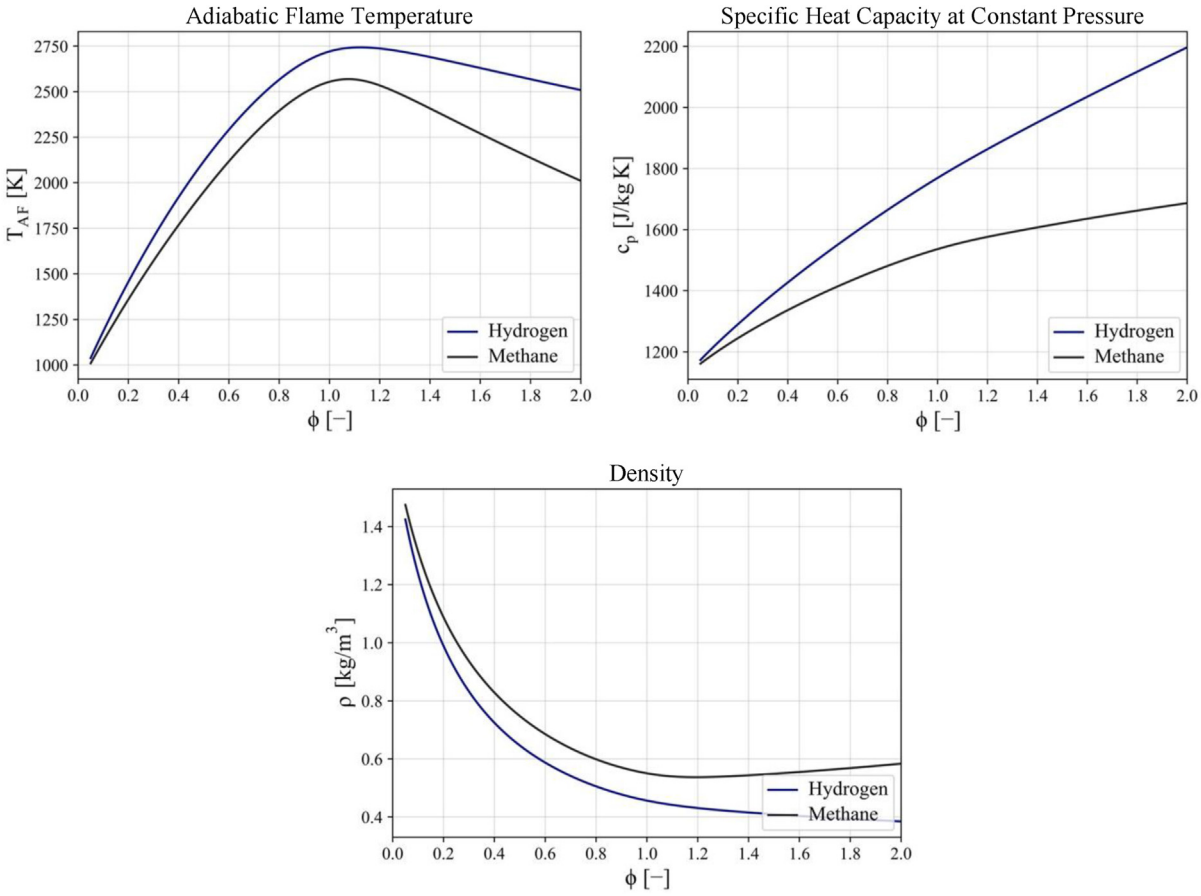

Fig. 1 – Flue gas properties in different equivalence ratios for burning methane and hydrogen with air at 4.3 bar and 610 K.

1.21 kg/m3 and a specific heat at a constant pressure of 1214.8 J/kg K.

To have an assessment of the case with pure hydrogen, first, it is assumed that the air enters the combustor with the same pressure and temperature. If the flue gas properties show a significant difference, it means the matching point will alter in a way that the original assumption was not correct. The hydrogen fuel rate is calculated based on equal heat input and 120 MJ/kg of LHV. This leads to 2.8 g/s of hydrogen which with assumed 0.8 kg/s of the air inlet, an equivalence ratio of 0.12 will be realized. The adiabatic temperature will be 1236.51 K with 1.18 kg/m^3 density and 1228.8 J/kg K of specific heat. All these values and the composition of products are provided in Table 2.

Table 2 – Flue gas properties comparison for methane and hydrogen. Air with 21% O_2 and 79% N_2 at 4.3 bar and 610 K.

Property	Methane	Hydrogen
Fuel flow rate for nominal power output	6.7 g/s	2.8 g/s
Air flow rate	0.8 kg/s	0.8 kg/s
Flue gas mass flow rate	0.8076 kg/s	0.8028 kg/s
Flue gas density	1.2046 kg/m^3	1.1815 kg/m^3
Flue gas flow rate	0.67 m^3/s	0.68 m^3/s
Stoichiometric air fuel ratio	17.12	34.06
Actual air fuel ratio	120	288
Equivalence ratio	0.14	0.12
Adiabatic flame temperature	1230.52 K	1236.51 K
Flue gas heat capacity at constant pressure	1214.8 J/kgK	1228.8 J/kgK
Mass fraction of N_2	0.75587	0.76423
Mass fraction of O_2	0.17352	0.20459
Mass fraction of H_2O	0.03138	0.03092
Mass fraction of CO_2	0.03834	0.00000
Mass fraction of NO and NO_2 (sum)	< 0.001	< 0.001

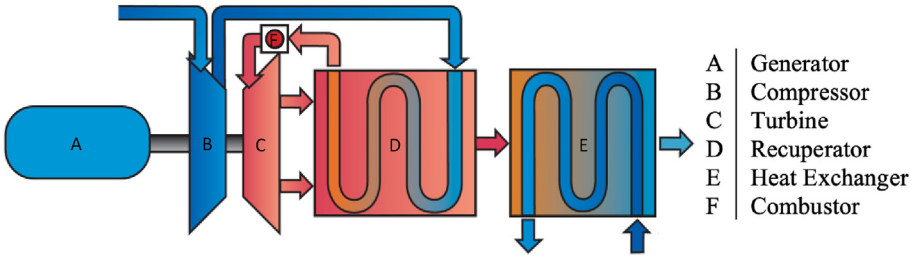

Fig. 2 – Schematic of the components in AE-T100 PH micro gas turbine.

Shifting the fuel from methane to hydrogen has increased the temperature by around 6° and with the changes in the density, the volumetric flow rate at the turbine is changed from 0.67 m^3/s to 0.68 m^3/s (a 1.5% increase). The specific heat capacity of the flue is increased by 1%. These minor changes are due to lean combustion ($\varphi < 0.15$) in the MGT, so the impact of fuel alteration on the composition of the flue gas is minor as the largest share of it is the excess air. For gas turbines with air to fuel ratios lower than MGTs, the variation of flow properties is expected to be higher [33].

Although the assessments were conducted using a reduced order model, it provides the basis for cycle evaluation, as they are also usually conducted by zero-dimensional or one-dimensional models. Even with this level of accuracy, it could be concluded that the fuel shift from methane to hydrogen will have a minor effect on the flow entering the turbine section and therefore only small variations in cycle points are expected thanks to the low fuel-air ratios in the MGT.

The following section presents an overview of the experimental setup of the micro gas turbine with details on the modifications implemented to enable running the engine with hydrogen blended fuel. Each of the challenges described previously has been addressed during the modifications described.

Development of Mgt running with hydrogen fuel

T100 PH micro gas turbine

The Turbec T100 PH micro gas turbine is a commercial engine used for the production of both power and heat. The engine consists of a single-stage centrifugal compressor, a single-stage radial turbine, and a single tubular combustor. It operates based on the regenerative Brayton cycle, where the heat from the hot gas that exits the turbine is transferred to the air entering the combustor via a recuperator. In addition to the recuperator, the engine is also equipped with a gas/water heat exchanger, which makes use of the remaining heat in the exhaust gas to warm up the recirculating water. The permanent magnet generator present in the engine enables it to run with a variable rotational speed.

To produce a desired power output, the controller of the T100 PH utilizes two main parameters: fuel flow rate and rotational speed. The engine is run to produce the demanded power, while maintaining the turbine outlet temperature below the maximum allowed value to prevent damage to the hot components of the engine due to high temperatures.

The Turbec T100 PH micro gas turbine has the capability to produce 100 kW of power at ISO conditions with a pressure ratio of 4.3, a turbine inlet temperature of 960 °C, and a rotational speed of 70,000 rpm. The engine operates within the range of power outputs and the controller manages this by adjusting the fuel flow rate and rotational speed. To ensure the endurance of the hot components in the engine, the turbine outlet temperature (TOT) must be maintained below a maximum allowed value of 645 °C, which is the nominal load. A schematic representation of the main components of the T100 PH unit can be seen in Fig. 2.

A T100 PH unit has been installed in the Risavika gas centre located in Stavanger, Norway. This unit has been the subject of various research projects in the past. The most recent program aimed to expand the operation of the micro gas turbine to a wider range of fuel types, including hydrogen-enriched fuels and ultimately pure hydrogen. To achieve this goal, the program was divided into two phases. In the first phase, a hydrogen content of up to 30% was achieved, while in the second phase, the operation was successful with a hydrogen content of up to 100% while still maintaining emissions below regulated limits. The modifications made to the system to accommodate the project are depicted in Fig. 3 and mainly consisted of changes to the fuel system, combustor, and controller. To evaluate the performance of the

Fig. 3 – Turbec T100 PH unit with modified combustor and fuel train for flexible fuel operation.

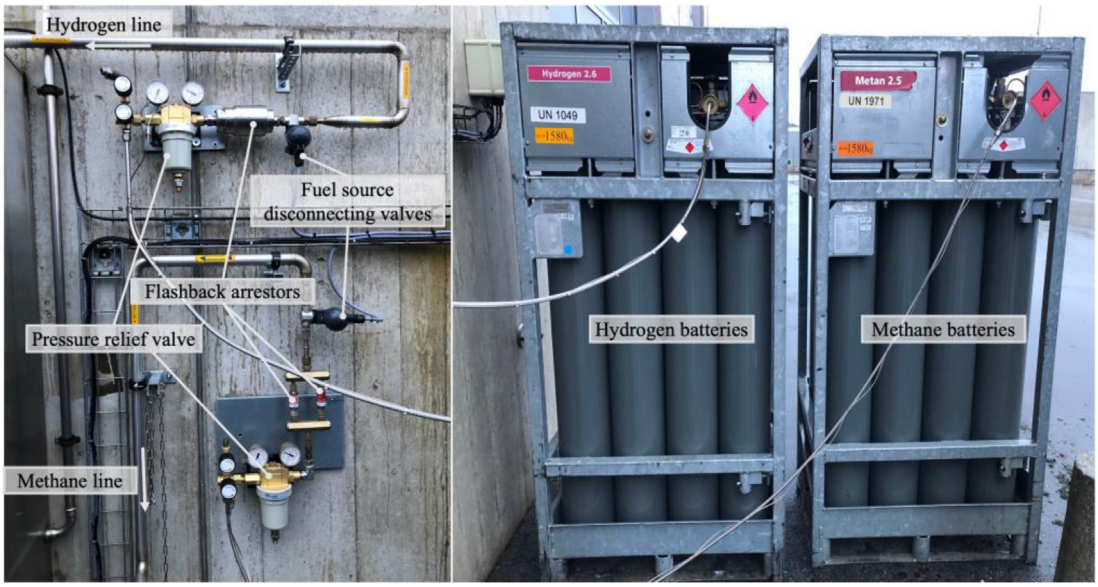

Fig. 4 – Fuel system arrangement outdoors, the valves left and fuel bottles right.

engine, numerous sensors were installed, and their readings were carefully monitored during the testing phase. Each of these modifications will be discussed in more detail in the sections that follow.

Fuel system

The original fuel system of the engines was designed to operate at low pressures, with an external compressor providing the necessary pressure boost. However, this system has been replaced with a new set-up that includes fuel sources such as methane and hydrogen batteries stored in a bundle structure. The pressure of the fuels is reduced using pressure relief valves and protected from flashbacks via arrestors. The fuel bundles and valves are located outside the building, with fuel disconnecting valves in place as a safety measure to cut the fuel supply in the event of a leak. The fuel bundles and valves can be seen in Fig. 4.

The new fuel train system is temporarily installed on the MGT and is depicted in Fig. 5. The system consists of separate lines for methane and hydrogen which are combined to form a mixture that is delivered to the engine. The engine operator controls the mass flow rates of both fuels to regulate the fuel ratio. The mixing station has larger diameters than the rest of the system and is designed to allow for adequate mixing of the fuels. The mixed fuel then passes through a safety valve and is divided into main and pilot lines. Initially, two main valves were installed for increased flexibility in control, but the experiments showed that only one main valve and one pilot valve were needed to function properly. The fuel is transmitted into the combustor through two lines, with a pilot in the middle and the main burners surrounding it. The main

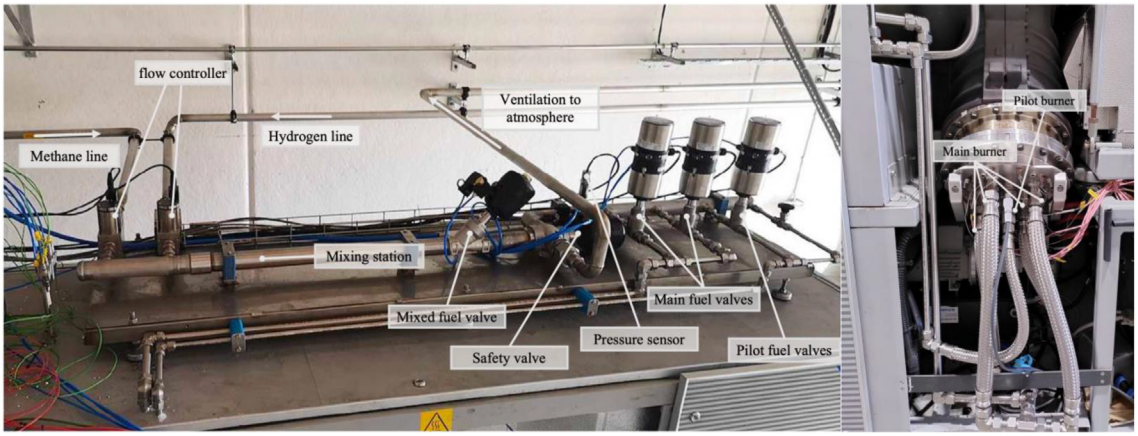

Fig. 5 – Fuel system indoors, the mixing station and fuel trained installed on top of the MGT enclosure, left, and the combustor, right.

Fig. 6 – Evolution of combustion chambers, a) Turbec, b) F400s ver.01 and c) F400s ver.02.

burner is composed of 10 single-jet nozzles that are supplied by four lines.

Combustor

The experiments utilized the F400s.3 combustion system developed by DLR, which consisted of two different flame tubes: ver.01, with the same length as the original combustor, and ver.02, with an extended flame tube. This combustion system was used as a replacement for the original Turbec swirl-type combustor. All of the experimental results reported in this work are based on variant (c) shown in Fig. 6.

Unlike the original combustor, the DLR F400's primary stage doesn't rely on swirl stabilization. Instead, it employs a stabilization principle that involves a combination of jet and recirculation, commonly referred to as the FLOX® concept. However, the pilot stage still uses the widely used swirl stabilization method. The swirler with annularly arranged air and fuel orifices directs fuel tangentially and axially into the pilot stage, thus enhancing mixing.

In the main stage, the nozzles allow for good premixing and homogenization of the air-and fuel stream flow before reaching the flame zone. This, in turn, enhances combustion stability and reduces peak temperatures, thereby minimizing the chances of NOx formation.

Fig. 7 illustrates the FLOX® combustor, which features ten separate nozzles arranged in a circular pattern around the combustor cross-sectional area and pilot dome to inject main stage air axially with high momentum. Fuel is injected coaxially inside each nozzle to enable controlled premixing. The air jet mantle serves as a shield, reducing the risk of flashback and delaying ignition to achieve lean equivalence ratios and lower combustion temperatures.

Flame stabilization is ensured through a recirculation zone developed by the air jets, where hot exhaust gases are transported back toward the root of the flame with negative axial

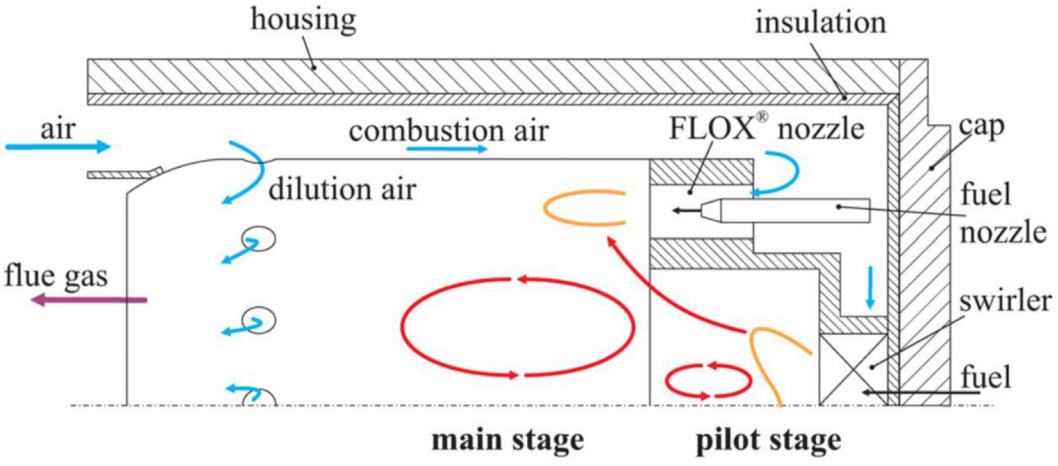

Fig. 7 – Schematic of the FLOX®-combustion principle [36].

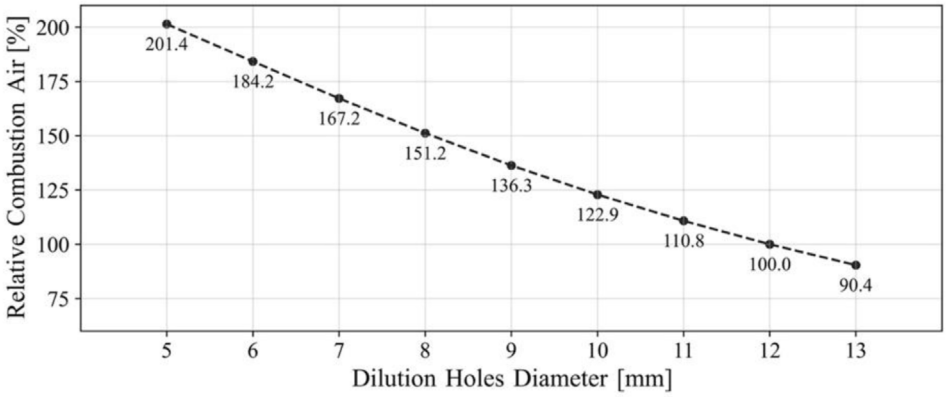

Fig. 8 – Expected relative combustion air over dilution hole diameter.

velocity. The developing flame is lifted off the combustor base to avoid excessive material stress inside the combustor head. More details about the combustor design and principle are available in Refs. [36,37].

The F400s.3 combustor is designed to operate with a range of fuels from low calorific synthesis gas up to natural gas. The combustor core underwent successful testing at DLR in an atmospheric test rig prior to the MGT test. The atmospheric tests were conducted with a gradual increase in hydrogen contents, up to pure hydrogen, to evaluate the fuel flexibility and performance of the optimized F400s combustor. To ensure that the velocity fields and jet velocities inside the combustor were comparable, the fuel input level and the supplied air were pressure-scaled. OH* chemiluminescence and emissions measurements were performed to assess stability and functionality [37]. Results indicated that stable flames were achieved across the fuel composition range tested, and no flashback or material problems were observed during the investigations. The optimized combustor demonstrated fuel flexibility and an increased operating range concerning NOx emissions. Nevertheless, the increased pressure level and higher volumetric energy density in the operational environment introduce new factors that affect combustor behaviour and were not captured by the atmospheric investigations at DLR. The tests conducted in this work extend the experiences to the real-use case and demonstrate the feasibility of the optimized combustor under operational conditions.

In a recuperated MGT, a significant [37] amount of air is used as dilution air to cool down the exhaust gases after combustion, making them manageable for the turbine. When operating with high hydrogen content, the air split between combustor core air and dilution air was adjusted to accommodate the changed conditions. The diameter of the dilution holes downstream of the combustion zone, which distribute the supplied air inside the combustor, was adjusted to achieve this. The spot-welded dilution ring with defined holes was switched to four different configurations investigated according to Fig. 8: 9 mm (quite lean), 11 mm (slightly leaner), 12 mm (the original syngas configuration), and 13 mm (slightly richer). As the hydrogen content increases, better performance of the leaner variants is expected, but there is a higher risk of a lean blowout of the flame. Optimal operating conditions for increased hydrogen content operation are expected to be much leaner compared to natural gas operation because the reactivity of hydrogen is significantly higher, along with the adiabatic and resulting flame temperature for a certain amount of air or equivalence ratio (see Fig. 1).

For all results approaching high hydrogen contents up to pure hydrogen, the 9 mm configuration was used, resulting in approximately 36% more air distributed to the combustion zone than in the original configuration. These values are based on rough estimations by resulting cross-sectional areas of the different significant holes or openings. This is expected to allow for low enough NOx emissions levels combined with sufficient flame stability margin.

Controller system

In addition to the new combustor design, modifications to the fuel controller were necessary to ensure the safe operation of the MGT with the ability to vary power and maintain emissions below the regulated values [38]. To accommodate the MGT to run on blended fuels, a new fuel delivery system was installed to provide the user-specified fuel mixture for the engine. To minimize changes to the engine controller, an additional fuel controller was added upstream from the MGT controller, which manages the fuel system before the MGT controller takes over. The modifications to the MGT controller are limited to adjustments in controller parameters to minimize changes to the existing system.

Fig. 9 presents the schematics of the micro gas turbine unit designed to operate with fuels containing high levels of hydrogen. The methane and hydrogen fuels are stored in bottles under pressures of up to 250 bar. The pressure is then reduced to 12–15 bar, which is set manually by the operator, through pressure relief valves. The fuel flow is then directed to flow controllers, where the mass flow rate of methane and hydrogen is regulated by the fuel train controller, an additional system. The purpose of this system is to supply the desired fuel mixture in accordance with the operator's specifications.

The mixed fuel enters a series of valves which are pneumatically controlled by the MGT controller. The first valve is a

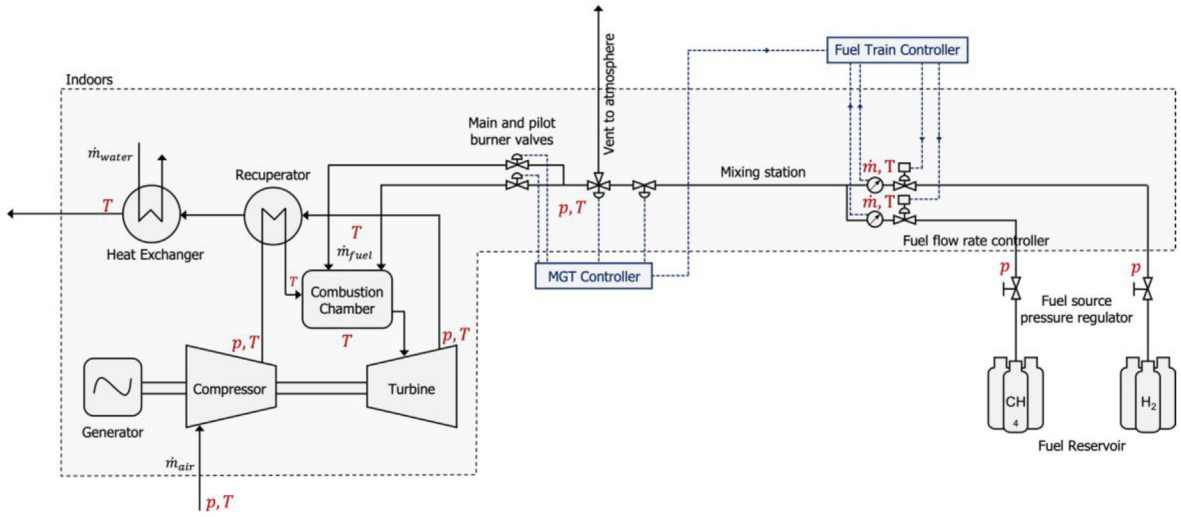

Fig. 9 – Structure of micro gas turbine unit equipped with the new fuel train system, controllers, and measurement points.

shutoff valve that connects the mixed fuel to the fuel train. After that, a 3-way valve is installed which provides a line to discharge the fuel to the atmosphere for safety reasons. The main path is divided into two separate lines and valves for the pilot and main fuel supply. The MGT controller regulates these valves to run the engine according to the operator's demand, the engine state (start-up, shut-down, steady, etc.), and the feedback from the engine sensors. Since the MGT controller has the primary control role, at the beginning of the operation it sends a signal to the fuel train controller to activate it. In Fig. 9 the connections between the controllers and valves are depicted. Moreover, the installed pressure, temperature, and flow rate sensors are also provided in red font. Some of these measurements are used by controllers and all of them are logged and collected for online monitoring of the operation and further post-process of the data.

The flammability range of hydrogen and methane poses a challenge in the fuel control system during the start-up. When starting the engine, the combustor runs at pilot mode where the valve for the pilot burner permits a high flow rate and then reduces to a lower value that remains unchanged through the operation. The pilot valve opening is regulated by the controller based on a map, with respect to the reference TOT and rotational speed of the engine, which are set by the engine's state and power set point. In Fig. 10 (a) the original mapping of the valve is presented. This setting is suitable for fuel blends with low hydrogen content. However, for high hydrogen content, the flammability limit of the fuel is reduced, therefore modifications are implemented to permit a stable start-up. The new mapping is shown in Fig. 10 (b), where a smoother transition is provided which is the successful pattern derived from a try-and-error procedure during the tests.

To see the effect of a valve adjustment, the start-up diagram for the engine before and after the pilot valve adjustment is illustrated in Figs. 11 and 12. The maximum pilot valve

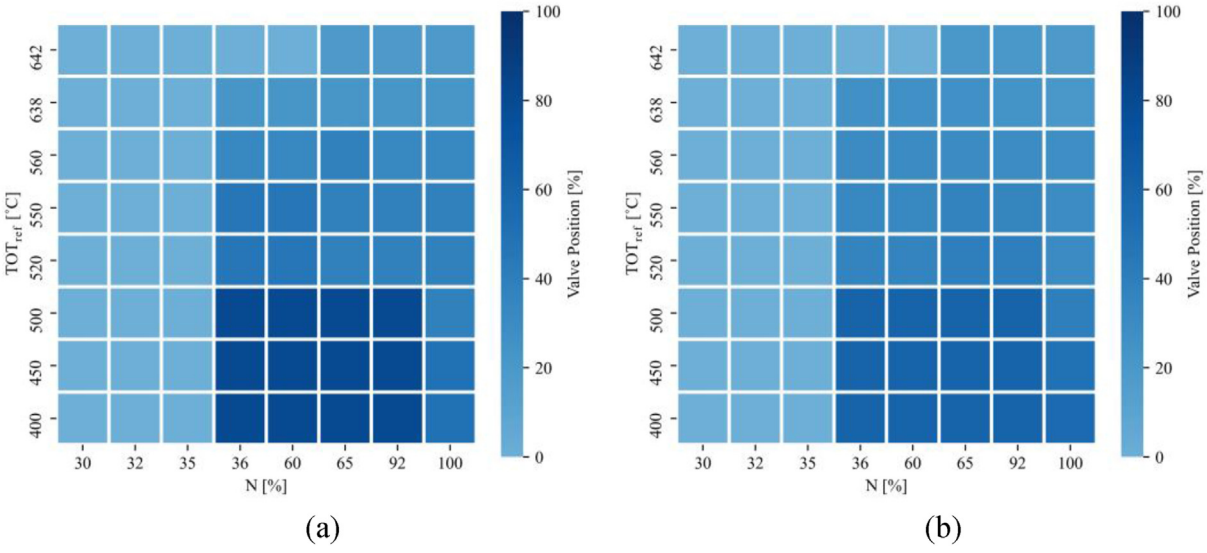

Fig. 10 – Pilot valve setting, (a) the reference settings, (b) modified settings.

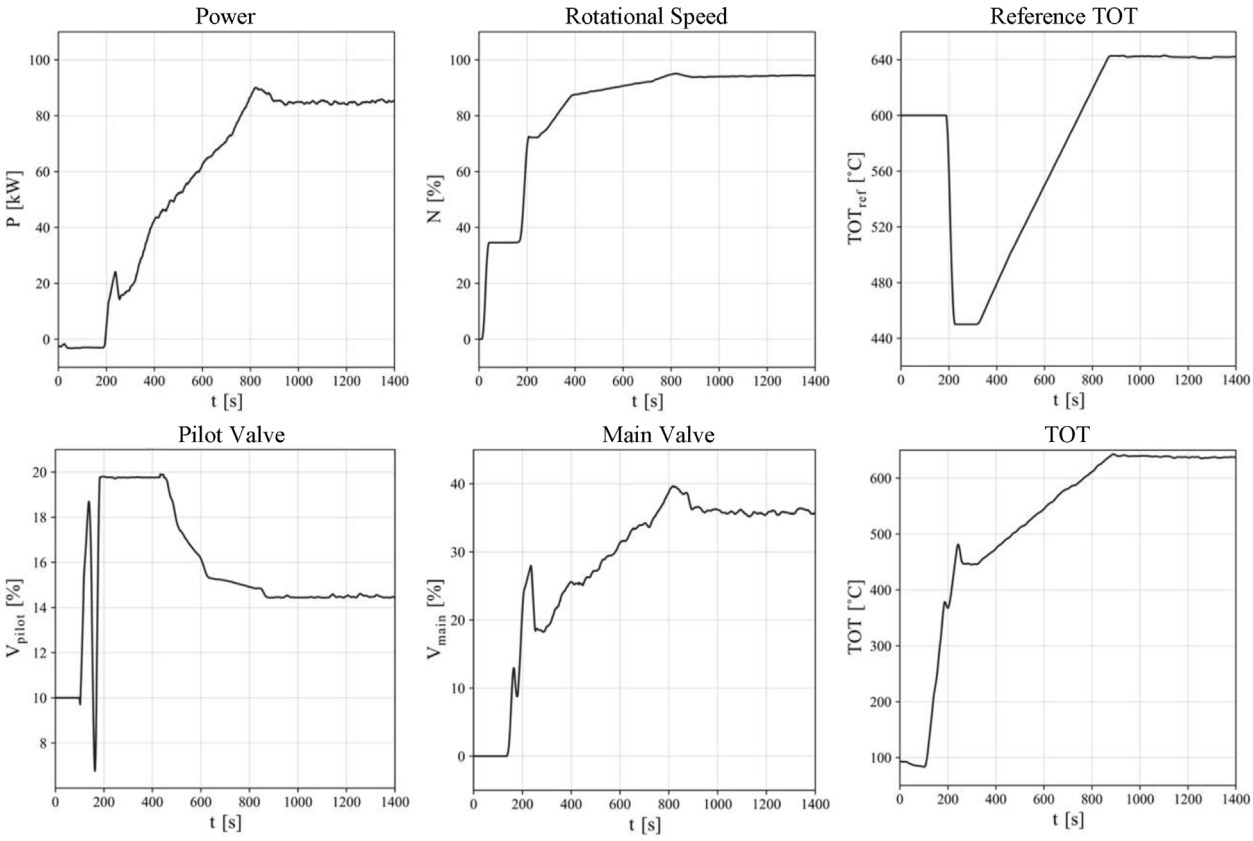

Fig. 11 – Start-up diagram for MGT before pilot valve adjustment. The hydrogen content in the fuel is 55% and the ambient condition during the test is 14 °C and 1.03 bar.

opening was 20% in the original setting which is reduced to around 14.5% for steady opening. These values are reduced to 17% and 10% after the adjustment which is visible in Fig. 10 (b). The pattern of reference TOT and rotational speed is also presented in both cases which are the parameters that pilot maps are based on. With these minor modifications in the start-up controller, the ignition and initial acceleration of the MGT were achieved without any difficulties.

Measurement system

To attain the most from the experiments, several additional sensors were installed at different locations of the engine. Sensors installed on the new fuel train are employed for controlling the fuel valves. Moreover, the combustion chamber as the new component of the engine is equipped with sensors so that its condition is constantly monitored during the test, trying to avoid high material temperatures. The pressure and temperature sensors inside the engine cycle are shown in Fig. 13 and a list of sensors measuring fuel properties is provided in Table 3. Hydrogen and methane properties are measured before and after mixing, as shown in Fig. 9. There is a thermocouple installed inside the combustor which measures the temperature of the fuel delivered to the combustor. The accuracy of sensors installed in the cycle and fuel system is presented in Table 4.

Out of 32 sensors listed in Figs. 13 and 6 sensors are built-in, and the rest are added for the purpose of the experiments. The temperature at the turbine inlet is measured by the thermocouples installed on the combustor, close to the flue gas exit from the combustor (Fig. 14 (a)). Other than the flue gas temperature, the metal temperature on both sides of the liner is also measured to monitor the component's condition. An example of such measurement is shown in Fig. 14 (b). The number of sensors installed on the combustor and their type and accuracy are described in Table 5.

To evaluate the effect of hydrogen injection on CO and NOx emissions a gas analyser is installed to measure the concentration of different components. The analyser's probe is installed on the way of exhaust gas (location 9 in Fig. 13). During the measurement phase, the exhaust gas emissions (NOx, CO, CO_2) are measured via the system shown in Fig. 15. The specification of the sensors in the analyser is provided in Table 6.

Results and discussion

Experiments have been conducted to realize the influence of enriching methane fuel with hydrogen, on the performance of a micro gas turbine and to investigate the influence of different amounts of hydrogen blend on the emissions and the stability of the combustion.

An initial setting was chosen for the new fuel train system, and it was tested. During the test runs in phase 1, unstable operations were observed, during which a better controller

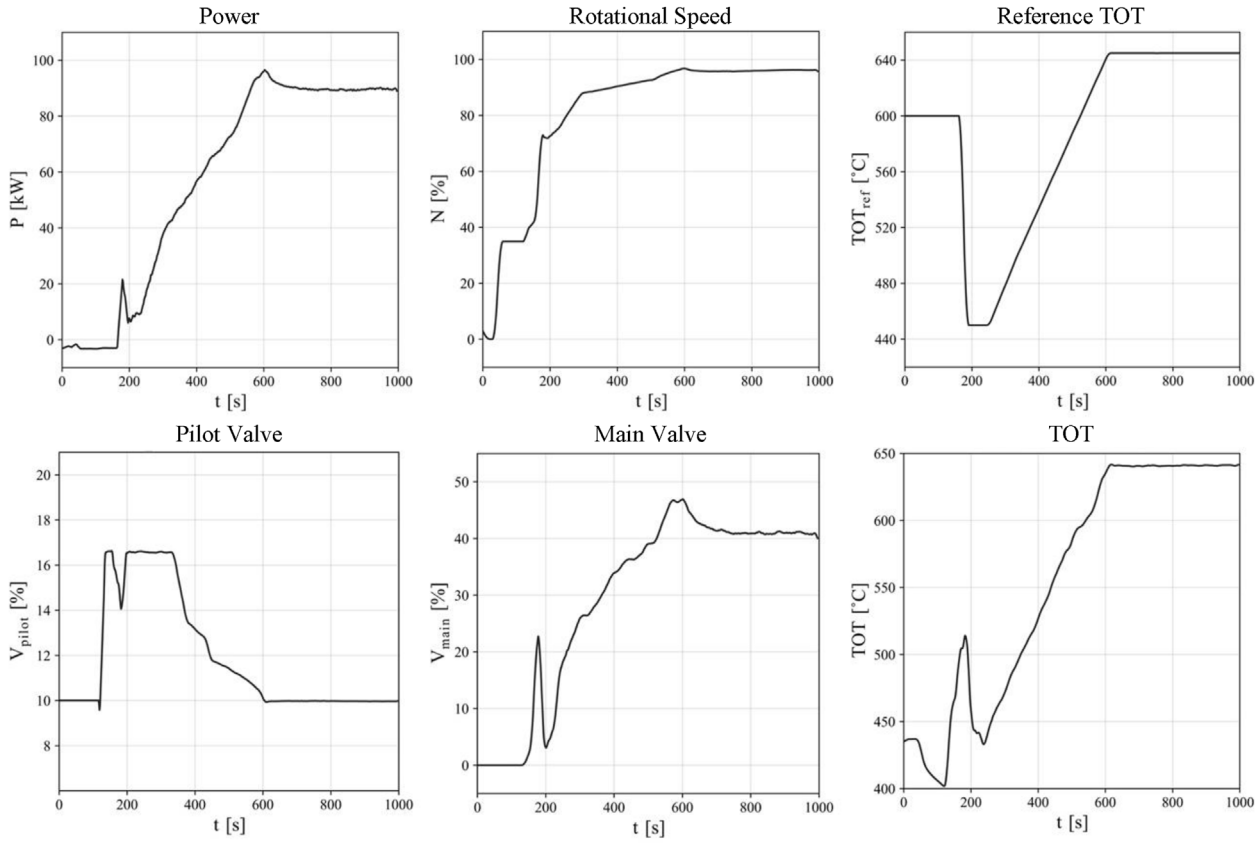

Fig. 12 – Start-up diagram for MGT before pilot valve adjustment. The hydrogen content in the fuel is 75% and the ambient condition during the test is 15 °C and 1.02 bar.

No.	Description	Temp.	Press.
1	Engine inlet	1	-
2	After inlet air filter	4	6
3	After compressor	3	3
4	After recuperator cold side	1	-
5	After combustor	2	-
6	After turbine	-	-
7	After diffuser	7	1
8	After recuperator hot side	-	-
9	Engine outlet	-	-
10	Before heat exchanger cold side	-	-
11	After heat exchanger cold side	4	-

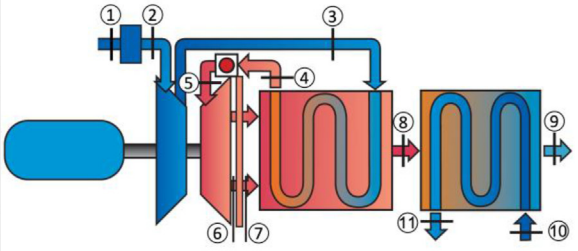

Fig. 13 – Cycle measurements, the table shows the number of installed sensors at each position.

Table 3 – Sensors installed on fuel system.

No.	Description	Temperature	Pressure	Mass flow rate
1	Methane fuel	1	1	1
2	Hydrogen fuel	1	1	1
3	Mixed fuel	1	2	–
4	Fuel in combustor	1	–	–

Table 4 – Performance of the installed sensors in the cycle and fuel system.

No.	Sensor	Accuracy
1	Temperature	±1.1 °C - 2.2 °C
2	Pressure	±0.3% of Full Scale
3	Mass flow rate	± (0.4% of Reading + 0.2% of Full Scale)

Fig. 14 – Examples of sensors installed in the combustion chamber, (a) flow temperature and (b) metal temperature.

setup was explored through a try-and-error manner. While this was effective for hydrogen content below 30%, for higher contents of hydrogen and especially in high power modes, the instabilities grew which were not controllable via fuel injection control.

During the second phase of the experiments, a modified version of the combustor was designed and manufactured by DLR, with smaller dilution holes to increase the airflow to the main burner and thereby imply more effective material cooling. Stable combustion was achieved in phase 2, thanks to the combustor setup. During a week of operation, blended fuel consisting of methane and hydrogen, with a high share of hydrogen (more than 50%) was fed to the engine, and different manoeuvres were conducted.

To illustrate the importance of the valve setting, operational results from the engine before and after valve adjustments are reported here. The normalized values reported in percentage points are calculated through the equations below, where P_{nom} and N_{nom} represent the power output and rotational speed of the engine at nominal conditions. $T_{comb,max}$ represents the maximum allowed temperature in the combustor and $T_{cooling\ air}$ is temperature of cooling air surrounding the combustion chamber.

$$P_{norm} = \frac{P}{P_{nom}} \tag{3}$$

$$N_{norm} = \frac{N}{N_{nom}} \tag{4}$$

$$T_{comb,norm} = \frac{T_{comb} - T_{cooling\ air}}{T_{comb,max} - T_{cooling\ air}} \tag{5}$$

Table 5 – Sensors installed on the combustor.

Description	No. Of sensors	Type	Accuracy
Metal temperature	9	Type N	±0.4%
Flue gas temperature	2	Type N	±0.4%
Inlet air temperature	1	Type N	±0.4%
Fuel temperature	1	Type N	±1.5 °C

Table 6 – Sensors in the gas analyser.

Item		Unit	Accuracy	Resolution
1	O_2	%	±0.8% of f.v.	0.01 vol%
2	CO	ppm	±2 ppm CO	1 ppm CO
3	NO	ppm	±2 ppm NO	0.1 ppm NO
4	NO_2	ppm	±5 ppm NO_2	0.1 ppm NO_2
5	CO_2	%	+1% of m.v.	0.01 vol% (0–25 vol%)
6	HC	ppm	±2% of m.v.	10 ppm

Fig. 16 displays the main operational parameters during a start-up and load variation test before the controller modifications were made. The test was run using a blended fuel consisting of approximately 55% hydrogen and 45% methane. A start-up to 85 kW was performed, and before reaching steady-state conditions, NOx emissions close to 18 ppm were observed and then reduced to 14.1 ppm at steady-state. When the power was increased to 100 kW, the NOx emissions rose to 15.7 ppm. The power was then reduced to 80 kW and increased again to 100 kW. During the second 100 kW load, the temperature of the flue gas was slightly higher and so were the NOx emissions. The fuel for the main burner was regulated by the main valve, which varied with the power output, while the opening of the pilot valve was almost constant throughout the operation. The shutdown from 100 kW was accompanied by changes in the fuel valve positions, and while the main valve was completely shut off, the pilot valve was reduced to 10%.

The experiments involving the micro gas turbine unit were conducted by increasing the hydrogen content in the fuel and running the engine at different power outputs. However, when the hydrogen content in the fuel exceeded 55%, instabilities during start-ups were observed along with high NOx emissions. To overcome this, modifications to the control parameters were made through a try-and-error process, which enabled safe operation in high hydrogen fuel mode with low emissions. The results from experiments with hydrogen content between 55% and 75% are missing due to a crash in the log system on one day and fuel leakage on another day. However, data from experiments with hydrogen content from 75% to 100% is available, and the effect of valve adjustments on the engine's performance is evident. Fig. 17 shows the engine's run with a hydrogen content of around 75%. The reason why the percentage of hydrogen is almost but not exactly equal to 75% is that the fuel controller is designed to receive hydrogen/methane mix ratios in mass bases, and the volume base mix depends on the density of the fuels, which can vary based on changes in pressure and temperature of the fuel.

The experiments continued by increasing the hydrogen content in the fuel and running the engine at different power levels. However, instabilities were observed during start-ups and high NOx emissions were recorded when the hydrogen content was above 55%. To address this, modifications to control parameters were made through a try-and-error process to allow safe operation in high hydrogen fuel mode with low emissions. The results from two days of runs with hydrogen content between 55% and 75% are missing due to a crash in the log system and fuel leakage. However, data from experiments with hydrogen content from 75% to 100% after

Fig. 15 – Exhaust gas composition measurements, probe installed on exhaust path in the left and analysing kit in the right.

the controller modifications are available. Fig. 17 shows the engine's run with approximately 75% hydrogen. During the manoeuvre, the engine was started successfully with 75% hydrogen and 90 kW power output, and the difference in operation with the new valve settings compared to before the controller adjustments (Fig. 16) was noticeable. The maximum pilot valve opening occurred during the start-up at 17% and was reduced to around 10% during the rest of the manoeuvre. The highest NOx emissions during the run were 14 ppm, which occurred during the power step up to 100 kW. This is compared to the previous setup where the NOx emissions were 19 ppm during the overshoot for a 100-kW load (Fig. 16).

Other than transient conditions, the steady-state data from 80-, 90-, and 100-kW power outputs could be compared from two controller settings. At 80 kW the normalized flue gas temperature was 88.9% with 13.3 ppm of NOx production, while the same parameters are 89.2% and 8.1 ppm in the new controller arrangements. Although the trend of the temperature of flue gas close to the combustor outlet is consistent with the NOx emissions, it is worth mentioning that NOx

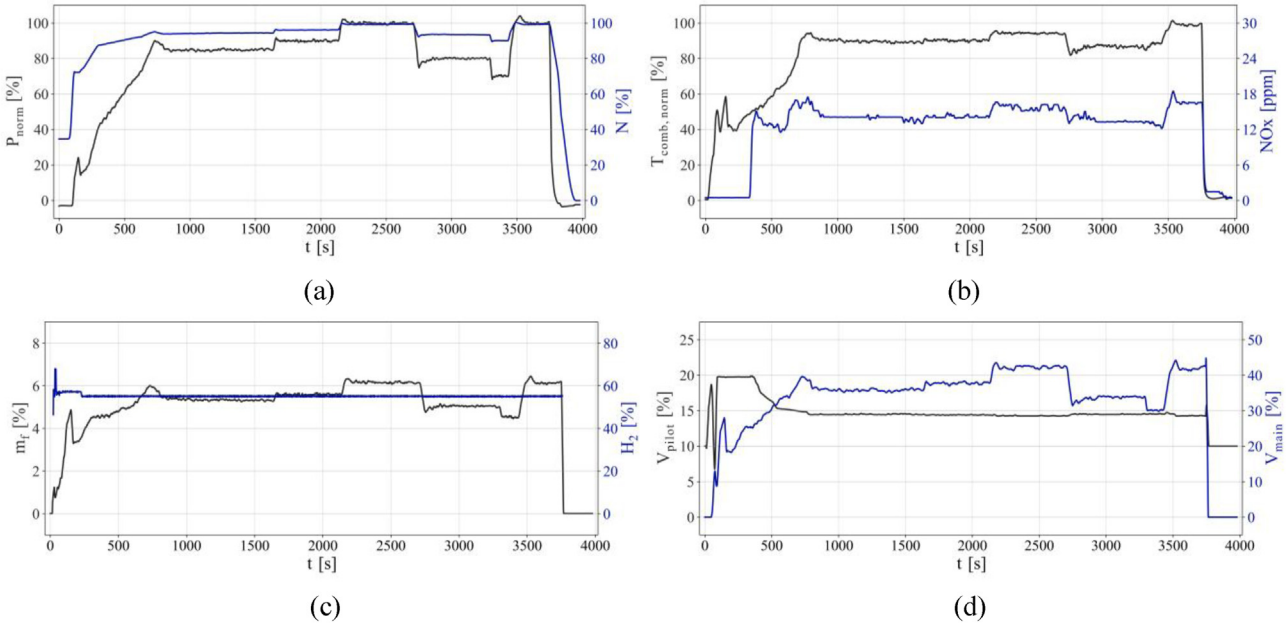

Fig. 16 – Start-up and power stepdown before adjusting the controller setup. The ambient temperature was 14 °C and the ambient pressure was 1.03 bar during the test.

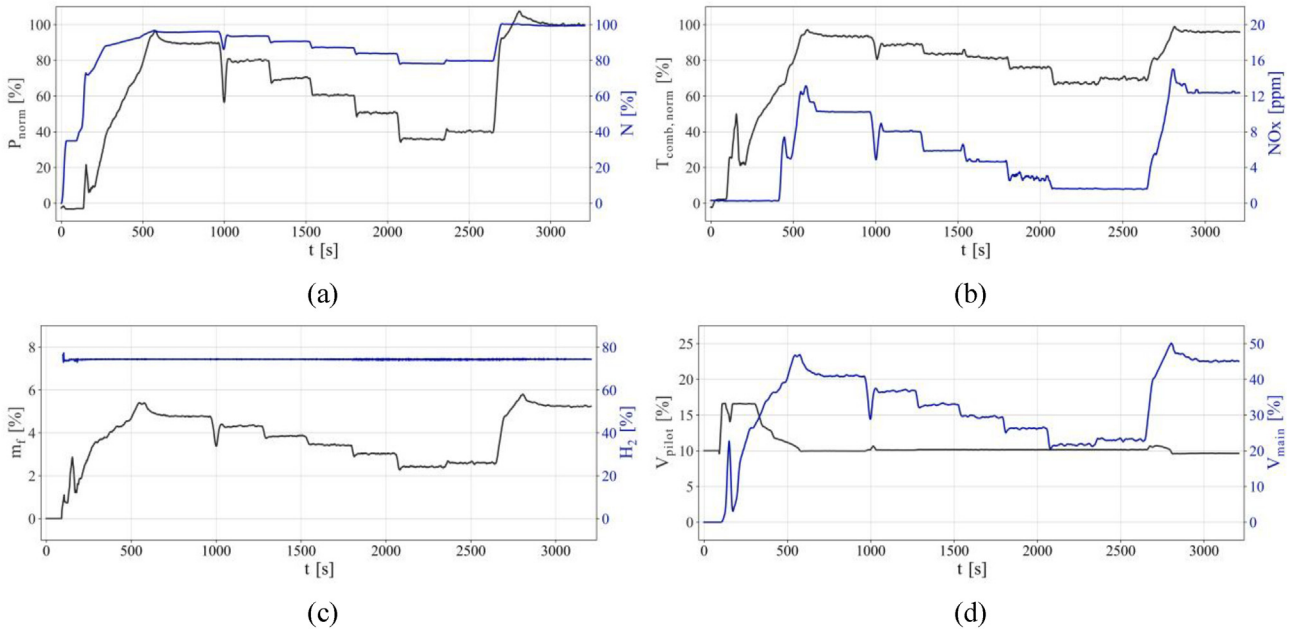

Fig. 17 – Power variation with F400-s ver02, modified controller setup. The ambient temperature was 15 °C and the ambient pressure was 1.02 bar during the test.

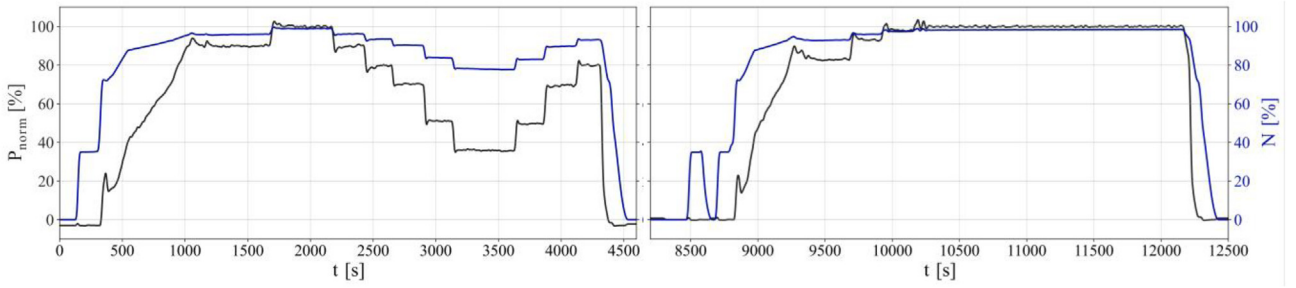

Fig. 18 – Power and rotational speed for manoeuvring with high hydrogen content.

production is a local phenomenon and more correlated to temperature in different regions of the combustor. The flue gas temperature presented here is also a value measured at a specific location. However, it could be used as an indicator of temperature increase or decrease in the combustor. For 90- and 100-kW power outputs, the NOx emissions after controller adjustments are 10.2 and 12.3 respectively while in previous arrangements the values were 14.1 for 90 kW and 15.7 and 16.5 for 100 kW. The adjustment of the pilot valve has not only provided a stable start-up and ignition but also helped to significantly reduce the NOx produced during the combustion.

After reaching a suitable setup for the controller, a series of experiments were conducted with an increasing share of hydrogen in the fuel, up to 100%. The whole test included 2 start-ups and shutdowns which lasted for 3 h and 30 min. The

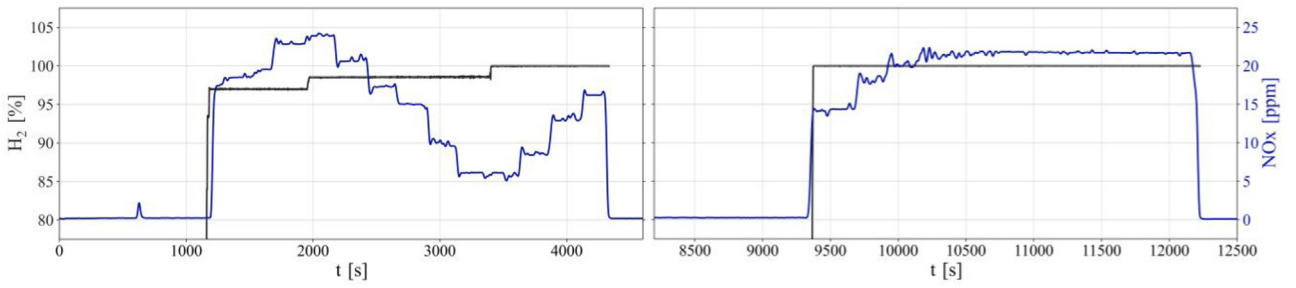

Fig. 19 – Hydrogen content and NOx emissions for manoeuvring with 100% hydrogen.

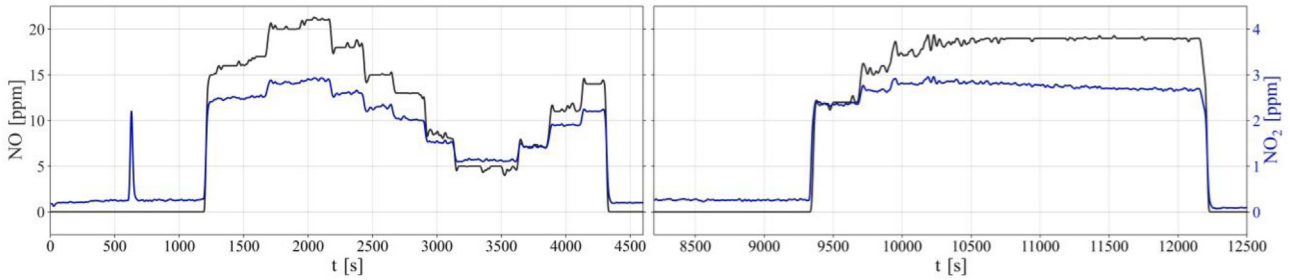

Fig. 20 – NO and NO_2 emissions for manoeuvring with 100% hydrogen.

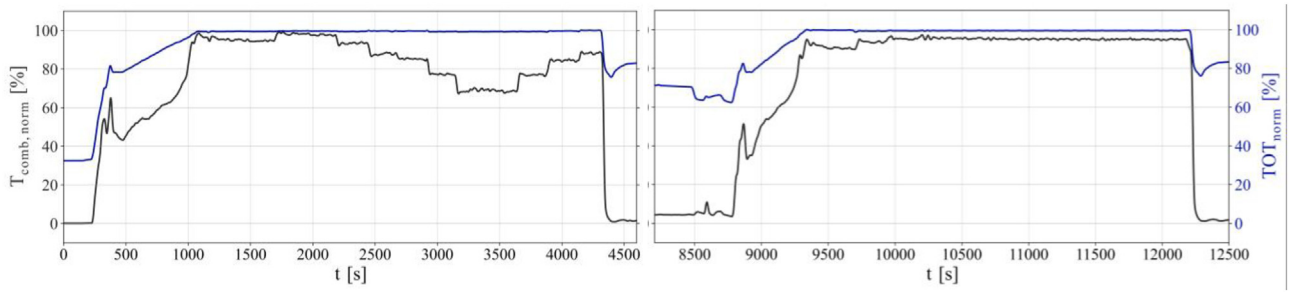

Fig. 21 – Combustor outlet temperature and turbine outlet temperature for manoeuvring with 100% hydrogen.

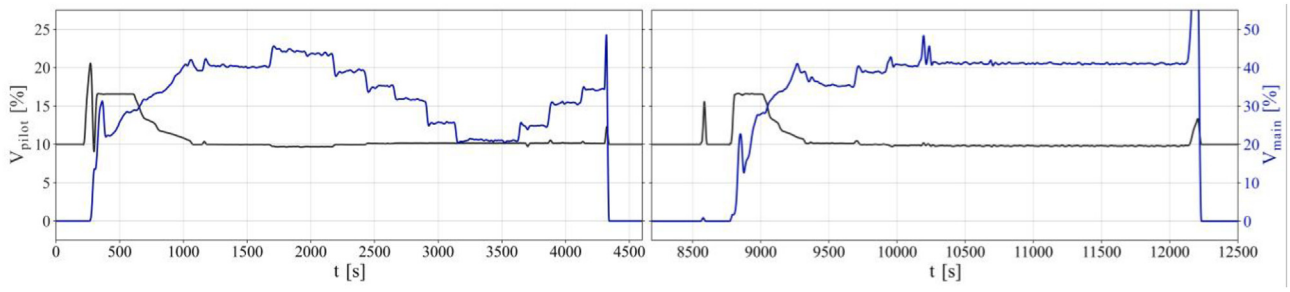

Fig. 22 – Fuel valves' position for manoeuvring with 100% hydrogen.

collected data are presented in Figs. 18–22. About an hour of data between two runs is eliminated in these figures, as it was only a cooling-down process for the engine. The initial ignition was successfully achieved with 90 kW of power with 97% hydrogen, with a smooth transition thanks to the optimized valves' positioning (Fig. 22). In about 10 min, the engine reached to 95.8% of its nominal rotational speed and produced 90 kW power with NOx productions of less than 20 ppm (Figs. 18 and 19). A 10 kW step-up was conducted after about 10 min to reach the maximum power of 100 kW. At this point, the rotational speed was elevated up to 98.9% of the nominal value and NOx emissions increased to 22.8 ppm (Figs. 18 and 19). Preserving the same power set point, hydrogen was added to the fuel to reach 98.5% concentration resulting 1.2 ppm increase in NOx emissions, presented in Fig. 19 and the share of NO and NO_2 production in NOx emissions is visible in Fig. 20.

After about 10 min of running at maximum power, the power was reduced to 35 kW in steps, without changing the

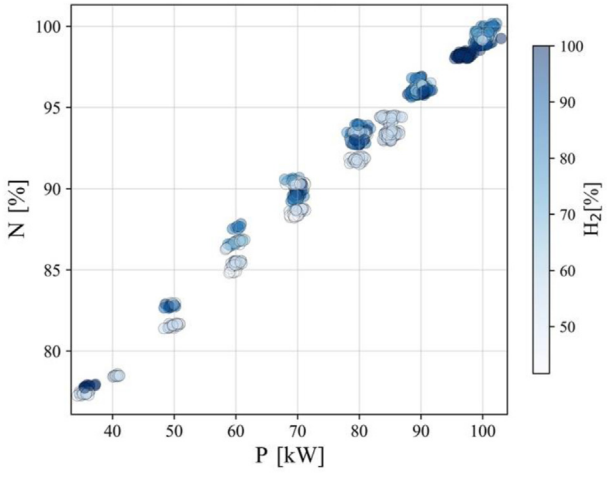

Fig. 23 – Engine rotational speed in different power output and different hydrogen content.

fuel blend. The NOx production was consequently reduced in steps to reach 6.1 ppm at 35 kW power. At this point, the hydrogen content was increased to 100% to examine the operation in low power output. The logged data presented in the figures show that only minor changes occurred in the engine when the hydrogen share was increased to 100%. With pure hydrogen, the power was increased to 50, 70, and 80, the same levels during the step-down with 98.5% hydrogen. Therefore, a comparison could be conducted; in all these tree levels, NOx emissions were 1~2 ppm lower than pure hydrogen. The amount of produced NOx during the load increase with pure hydrogen is lower than step-downs with 98.5% hydrogen. According to Fig. 20, this behaviour was attributed to lower NO which could be due to hysteresis effects, since a step up in power (and with it increasing NOx values) was compared with a step-down manoeuvre, hence decreasing NOx values.

The MGT was shut down while producing 80 kW with pure hydrogen. After waiting for an hour for the engine to cool down, a start-up to 80 kW was initiated with pure hydrogen. In that case, NOx emissions were slightly lower than 80 kW power rates during two previous 80 kW hits which are due to lower NO production according to Fig. 20. Since a similar behaviour has been observed by the authors for hot restarts, this might be an indication of a short cool-down which entails hot-start settings for the engine controller.

With three small steps, the power is increased to 100 kW, where a stable operation is achieved with pure hydrogen with NOx emissions of 21.9 ppm. With time passing, the rate of NO_2 production decreased and the total NOx produced decreased to 21.7 ppm. After about 45 min of running the engine with pure fuel at maximum power, the engine was safely shut down. The value of TOT is normalized based on Eq. (6) below, where TOT_{nom} is the turbine outlet temperature at nominal conditions (temperatures in Kelvin):

$$TOT_{norm} = \frac{TOT}{TOT_{nom}} \quad (6)$$

In Fig. 23, the relationship between rotational speed and power output is shown after the transient time spans were removed from the data collected from different engine manoeuvres. The TOT (total temperature of the cycle) of the engine is also considered in evaluating the effect of fuel variation on the engine's steady-state operation. The rotational speed of the engine at various power rates exhibits a linear relationship with power output, which is the expected pattern from the engine as previously observed when running on fossil fuels. The highest power output of 100 kW was reached with hydrogen content ranging from 55% to 100%, and as seen in Fig. 23, the range of fuel is almost at the same rotational speed. However, slight deviations in rotational speed can be observed in the figure, for instance at 60 kW, mainly due to the fact that they were collected from different experiments carried out on different days with varying ambient temperatures.

Another cycle parameter indicating the controller's performance is the steady-state condition in turbine outlet temperature, which is provided in Fig. 24, again from all manoeuvres by filtering the transient time spans. In Fig. 24 (a) the amount of hydrogen content in the fuel is presented by colour and as it is visible, the hydrogen content does not seem to have a correlation with TOT. Note that the relative share of hydrogen in the figures is calculated on a volume basis. For instance, at 100 kW higher hydrogen contents have resulted in lower TOT values while the opposite could be observed at 80 kW. This is also the effect of ambient temperature, as illustrated in Fig. 24 (b), higher TOT values are developed in the cycle when the environment was warmer.

The rate of NOx production in all power production rates with different hydrogen content is illustrated in Fig. 25. As it is evident from this figure, the rate of NOx emissions is directly correlated with an increase in hydrogen content and power rate, as both will increase the temperature in the combustion chamber. Therefore, moving to the upper right part of the graph, the darker the markers become, except for the data from 55% hydrogen which is not in compliance with this trend. The data from 55% hydrogen is from the experiments

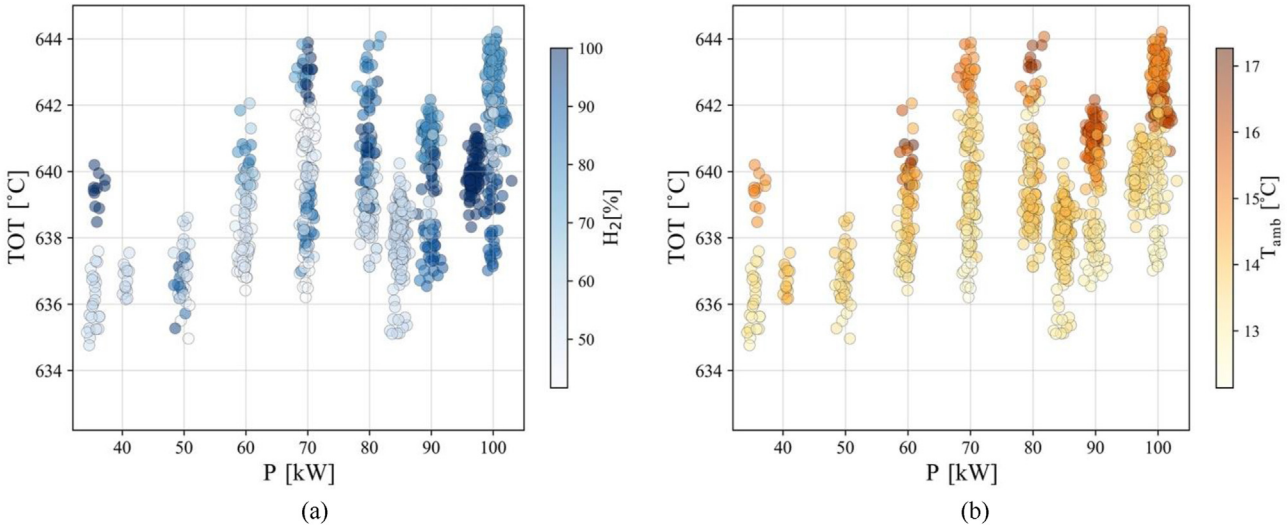

Fig. 24 – Turbine outlet temperature in different power output, (a) effect of hydrogen content and (b) effect of ambient temperature.

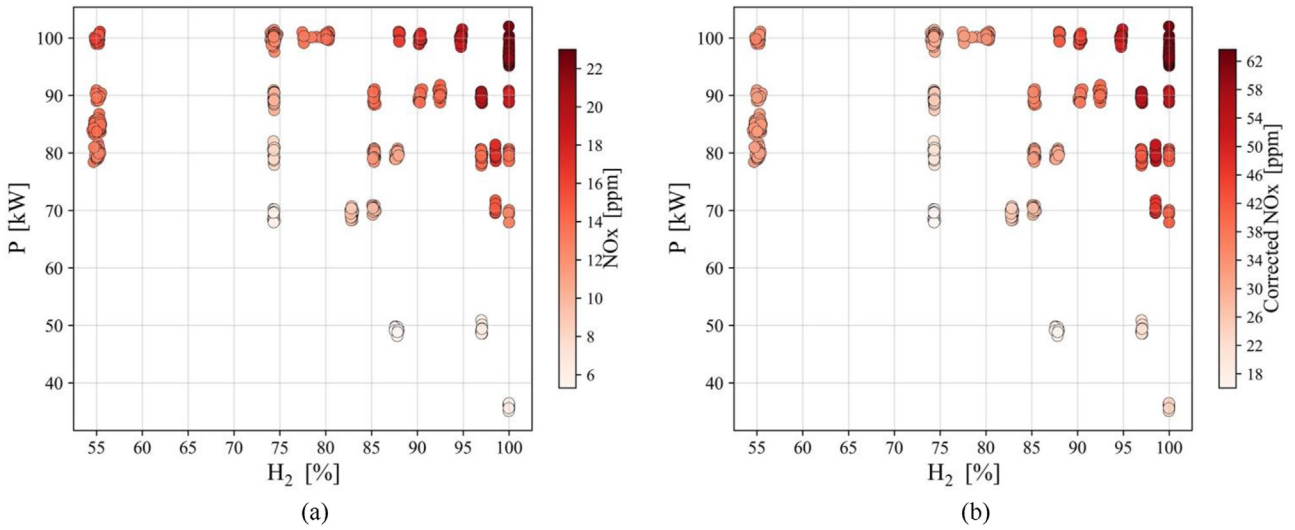

Fig. 25 – Effect of hydrogen content on NOx emissions in different power output (a) measured values (b) corrected values based on 15% oxygen case.

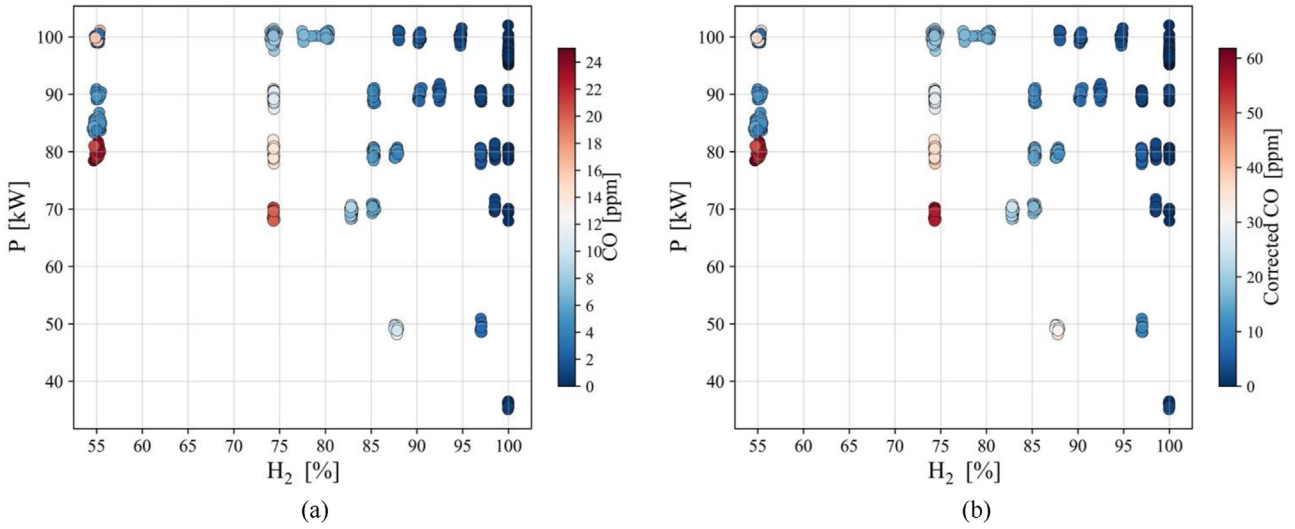

Fig. 26 – Effect of hydrogen content on CO emission in different power output(a) measured values (b) corrected values based on 15% oxygen case.

before valve adjustments. Fig. 25 shows how the valve adjustments are essential to control the emissions; as the coloring suggests, the NOx emissions at 100 kW with 55% hydrogen before valve adjustments are close to the case of running with 87% hydrogen and producing 100 kW after optimizing the valve settings.

To be able to compare the emissions against different combustion systems, the concentration of NOx and CO is corrected based on the case with 15% O_2 in the exhaust gas, as a standard. For this purpose, the measured emissions are corrected using Eq. (3) and the corrected values are illustrated beside the actual values (Figs. 25 and 26).

$$X_{corr} = X_{meas}\left(\frac{20.95 - 15}{20.95 - O_{2,meas}}\right) \quad (3)$$

It is expected that increasing hydrogen content in the fuel will reduce the rate of CO and CO_2 production. The concentration of CO and CO_2 is measured in flue gas and presented in Figs. 26 and 27 over a range of experimented power output and fuel blends. With pure hydrogen combustion, concentrations of CO and CO_2 in the flue gas are zero. With less hydrogen content the rate of carbon monoxide and carbon dioxide production increases. Looking at Fig. 26, it can be realized that

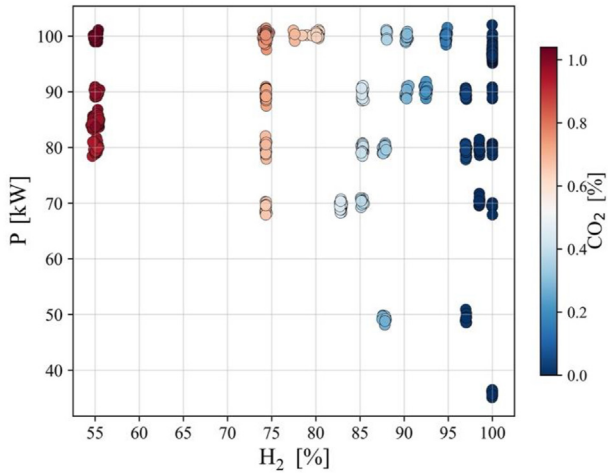

Fig. 27 – Effect of hydrogen content on CO_2 emission in different power output.

at constant fuel mix (for instance 75% hydrogen), the rate of CO production is higher at lower powers, which indicates nonideal combustion in low powers.

Conclusions

In this paper, the objective was to explore the potential of using hydrogen as an alternative fuel for carbon-free power generation in gas turbines. The challenges of using hydrogen as fuel include its less stable combustion and a higher likelihood of flashbacks, as well as higher generation of NOx emissions due to its higher combustion temperatures. The study presented the process of modifying a micro gas turbine originally designed to run on natural gas, to run on hydrogen-enriched fuel, and eventually pure hydrogen. The modifications involved the combustor, fuel train, and controller components. These modifications enabled the safe operation of the turbine while ensuring the emissions remained below regulated values.

The micro gas turbine was developed to run on hydrogen-enriched fuel up to 100% pure hydrogen. To achieve stable operation throughout the full range of power outputs, modifications were made to the combustor, fuel train, and controller. During the tests, the volume-based hydrogen content in the fuel varied from 40% to 100%, and the results showed a steady operation of the micro gas turbine with NOx emissions below the regulated limits. The highest NOx emissions recorded for pure hydrogen and full-load operation was 22 ppm, which equates to 62 ppm of the corrected value based on a reference of 15% oxygen in the exhaust gas. The full range of operation results with different hydrogen contents is presented, demonstrating the stability of the micro gas turbine while meeting the regulatory NOx emission requirements.

Declaration of competing interest

The authors declare that they have no known competing financial interests or personal relationships that could have appeared to influence the work reported in this paper.

Acknowledgments

This project has received funding from the European Union's Horizon 2020 research and innovation program under the Marie Skłodowska-Curie grant agreement No. 861079 ("Next MGT").The authors would like to express their sincere gratitude to Bjarte Ludvig Hetlelid for his exceptional contribution to the experiments conducted in this technical paper.

REFERENCES

[1] Little AD. Opportunities for micropower and fuel cell gas turbine hybrid systems in industrial applications - DOE report No. 85X-TA009V. 2000. Cambridge, Massachusetts 02140-2390 U.S.A., Jan. 2000.
[2] Yang J, et al. Thermodynamic modelling and real-time control strategies of solar micro gas turbine system with thermochemical energy storage. J Clean Prod Jul. 2021;304:127010. https://doi.org/10.1016/J.JCLEPRO.2021.127010.
[3] Best T, Finney KN, Ingham DB, Pourkashanian M. CO2-enhanced and humidified operation of a micro-gas turbine for carbon capture. J Clean Prod Mar. 2018;176:370–81. https://doi.org/10.1016/J.JCLEPRO.2017.12.062.
[4] Tang C, Zhang Y, Huang Z. Progress in combustion investigations of hydrogen enriched hydrocarbons. Renew Sustain Energy Rev Feb. 2014;30:195–216. https://doi.org/10.1016/J.RSER.2013.10.005.
[5] Zhang Y, Davis D, Brear MJ. The role of hydrogen in decarbonizing a coupled energy system. J Clean Prod Apr. 2022;346:131082. https://doi.org/10.1016/J.JCLEPRO.2022.131082.
[6] Morris JD, Symonds RA, Ballard FL, Banti A. Combustion aspects of application of hydrogen and natural gas fuel mixtures to MS9001E DLN-1 gas turbines at elsta plant, Terneuzen, The Netherlands. In: Proceedings of the ASME turbo expo. Stockholm: American Society of Mechanical Engineers Digital Collection; Dec. 1998. https://doi.org/10.1115/98-GT-359.
[7] Shih HY, Liu CR. A computational study on the combustion of hydrogen/methane blended fuels for a micro gas turbines. Int J Hydrogen Energy Sep. 2014;39(27):15103–15. https://doi.org/10.1016/J.IJHYDENE.2014.07.046.
[8] Imteyaz BA, Nemitallah MA, Abdelhafez AA, Habib MA. Combustion behavior and stability map of hydrogen-enriched oxy-methane premixed flames in a model gas turbine combustor. Int J Hydrogen Energy Aug. 2018;43(34):16652–66. https://doi.org/10.1016/J.IJHYDENE.2018.07.087.
[9] Rajpara P, Shah R, Banerjee J. Effect of hydrogen addition on combustion and emission characteristics of methane fuelled upward swirl can combustor. Int J Hydrogen Energy Sep. 2018;43(36):17505–19. https://doi.org/10.1016/J.IJHYDENE.2018.07.111.
[10] Minakawa K, Miyajima T, Yuasa S. Development of a hydrogen-fueled micro gas turbine with a lean premixed combustor. In: 33rd joint propulsion conference and exhibit. American Institute of Aeronautics and Astronautics Inc, AIAA; 1997. p. 1–6. https://doi.org/10.2514/6.1997-3388.

[11] Cappelletti A, Martelli F. Investigation of a pure hydrogen fueled gas turbine burner. Int J Hydrogen Energy Apr. 2017;42(15):10513–23. https://doi.org/10.1016/J.IJHYDENE.2017.02.104.
[12] Horikawa A, Okada K, Wirsum M, Funke HH-W, Kusterer K. 100% hydrogen dry low NOx combustor developments for 2MW class gas turbine. In: The proceedings of the international conference on power engineering (ICOPE). The Japan Society of Mechanical Engineers; 2021. https://doi.org/10.1299/JSMEICOPE.2021.15.2021-0222.
[13] Funke HHW, Beckmann N, Keinz J, Horikawa A. 30 Years of dry-low-NOx micromix combustor research for hydrogen-rich fuels - an overview of past and present activities. J Eng Gas Turbines Power Jul. 2021;143(7). https://doi.org/10.1115/1.4049764/1096348.
[14] Banihabib R, Assadi M. Dynamic modelling and simulation of a 100 kW micro gas turbine running with blended methane/hydrogen fuel. In: Industrial and cogeneration; manufacturing materials and metallurgy; microturbines, turbochargers, and small turbomachines; oil & gas applications, vol. 7. American Society of Mechanical Engineers Digital Collection; Jun. 2022. https://doi.org/10.1115/GT2022-81276.
[15] Perry RH, Green DW, Maloney JO. Perry's chemical engineers' handbook. 7th ed. New York: McGraw-Hill; 1997.
[16] Verhelst S, Wallner T. Hydrogen-fueled internal combustion engines. Prog Energy Combust Sci Dec. 2009;35(6):490–527. https://doi.org/10.1016/J.PECS.2009.08.001.
[17] Guo H, Smallwood GJ, Liu F, Ju Y, Gülder ÖL. The effect of hydrogen addition on flammability limit and NOx emission in ultra-lean counterflow CH4/air premixed flames. Proc Combust Inst Jan. 2005;30(1):303–11. https://doi.org/10.1016/J.PROCI.2004.08.177.
[18] Frenillot JP, Cabot G, Cazalens M, Renou B, Boukhalfa MA. Impact of H2 addition on flame stability and pollutant emissions for an atmospheric kerosene/air swirled flame of laboratory scaled gas turbine. Int J Hydrogen Energy May 2009;34(9):3930–44. https://doi.org/10.1016/J.IJHYDENE.2009.02.059.
[19] Ren JY, Qin W, Egolfopoulos FN, Mak H, Tsotsis TT. Methane reforming and its potential effect on the efficiency and pollutant emissions of lean methane-air combustion. Chem Eng Sci Mar. 2001;56(4):1541–9. https://doi.org/10.1016/S0009-2509(00)00381-X.
[20] Chong CT, Ng J-H. Combustion performance of biojet fuels. In: Biojet fuel in aviation applications. Elsevier; 2021. p. 175–230. https://doi.org/10.1016/B978-0-12-822854-8.00002-0.
[21] Jithin Ev, Varghese RJ, Velamati RK. Experimental and numerical investigation on the effect of hydrogen addition and N2/CO2 dilution on laminar burning velocity of methane/oxygen mixtures. Int J Hydrogen Energy Jun. 2020;45(33):16838–50. https://doi.org/10.1016/J.IJHYDENE.2020.04.105.
[22] Sun Y, et al. Effect of hydrogen addition on the combustion and emission characteristics of methane under gas turbine relevant operating condition. Fuel Sep. 2022;324:124707. https://doi.org/10.1016/J.FUEL.2022.124707.
[23] Zhou Q, Cheung CS, Leung CW, Li X, Li X, Huang Z. Effects of fuel composition and initial pressure on laminar flame speed of H2/CO/CH4 bio-syngas. Fuel Feb. 2019;238:149–58. https://doi.org/10.1016/J.FUEL.2018.10.106.
[24] Amar H, Abdelbaki M, Fouzi T, Zeroual A. Effect of the addition of H2 and H2O on the polluting species in a counter-flow diffusion flame of biogas in flameless regime. Int J Hydrogen Energy Feb. 2018;43(6):3475–81. https://doi.org/10.1016/J.IJHYDENE.2017.11.159.
[25] Xiang L, Jiang H, Ren F, Chu H, Wang P. Numerical study of the physical and chemical effects of hydrogen addition on laminar premixed combustion characteristics of methane and ethane. Int J Hydrogen Energy Aug. 2020;45(39):20501–14. https://doi.org/10.1016/J.IJHYDENE.2019.11.040.
[26] Toof JL. A model for the prediction of thermal, prompt, and fuel NOx emissions from combustion turbines. J Eng Gas Turbines Power Apr. 1986;108(2):340–7. https://doi.org/10.1115/1.3239909.
[27] Cowell LH, Smith KO. Development of a liquid-fueled, lean-premixed gas turbine combustor. J Eng Gas Turbines Power Jul. 1993;115(3):554–62. https://doi.org/10.1115/1.2906743.
[28] Ditaranto M, Heggset T, Berstad D. Concept of hydrogen fired gas turbine cycle with exhaust gas recirculation: assessment of process performance. Energy Feb. 2020;192:116646. https://doi.org/10.1016/J.ENERGY.2019.116646.
[29] Venkataraman KK, Preston LH, Simons DW, Lee BJ, Lee JG, Santavicca DA. Mechanism of combustion instability in a lean premixed dump combustor. J Propul Power May 2012;15(6):909–18. https://doi.org/10.2514/2.5515.
[30] Candel S. Combustion dynamics and control: progress and challenges. Proc Combust Inst Jan. 2002;29(1):1–28. https://doi.org/10.1016/S1540-7489(02)80007-4.
[31] Lee IB, Woo IS, Lee MC. Effects of nitrogen dilution on the NOxand CO emission of H2/CO/CH4syngases in a partially-premixed gas turbine model combustor. Int J Hydrogen Energy Sep. 2016;41(35):15841–51. https://doi.org/10.1016/J.IJHYDENE.2016.04.131.
[32] Juste GL. Hydrogen injection as additional fuel in gas turbine combustor. Evaluation of effects. Int J Hydrogen Energy Nov. 2006;31(14):2112–21. https://doi.org/10.1016/J.IJHYDENE.2006.02.006.
[33] Gülen SC. Gas turbines for electric power generation. 1st ed. Cambridge University Press; 2019.
[34] Chiesa P, Lozza G, Mazzocchi L. Using hydrogen as gas turbine fuel. J Eng Gas Turbines Power Jan. 2005;127(1):73–80. https://doi.org/10.1115/1.1787513.
[35] Goodwin DG, Moffat H, Speth RL. Cantera: an object-oriented software toolkit for chemical kinetics, thermodynamics, and transport processes. 2016. Version 2.2.1.
[36] Zornek T, Mosbach T, Aigner M. Optical measurements of a lower calorific values-combustor operated in a micro gas turbine with various fuel compositions. J Eng Gas Turbines Power Apr. 2019;141(4). https://doi.org/10.1115/1.4040908.
[37] Bower HE, Schwärzle A, Grimm F, Zornek T, Kutne P. Experimental analysis of a micro gas turbine combustor optimized for flexible operation with various gaseous fuel compositions. J Eng Gas Turbines Power Mar. 2020;142(3). https://doi.org/10.1115/1.4044901.
[38] Funke HH-W, Keinz J, Börner S, Hendrick P, Elsing R. Testing and analysis of the impact on engine cycle parameters and control system modifications using hydrogen or methane as fuel in an industrial gas turbine, vol. 8; 2016. p. 409–26. https://doi.org/10.1051/EUCASS/201608409.